

Dynamic recrystallization kinetics of as-cast AZ91D alloy

Yan XU^{1,2}, Lian-xi HU¹, Yu SUN¹

1. School of Materials Science and Engineering, Harbin Institute of Technology, Harbin 150001, China;

2. School of Mechanical Engineering, Beihua University, Jilin 132021, China

Received 24 July 2013; accepted 5 November 2013

Abstract: The flow behavior and dynamic recrystallization (DRX) behavior of an as-cast AZ91D alloy were investigated systematically by applying the isothermal compression tests in temperature range of 220–380 °C and strain rate range of 0.001–1 s⁻¹. The effect of temperature and strain rate on the DRX behavior was discussed. The results indicate that the nucleation and growth of dynamic recrystallized grains easily occur at higher temperatures and lower strain rates. To evaluate the evolution of dynamic recrystallization, the DRX kinetics model was proposed based on the experimental data of true stress–true strain curves. It was revealed that the volume fraction of dynamic recrystallized grains increased with increasing strain in terms of S-curves. A good agreement between the proposed DRX kinetics model and microstructure observation results validates the accuracy of DRX kinetics model for AZ91D alloy.

Key words: AZ91D magnesium alloy; compression; flow behavior; dynamic recrystallization behavior; kinetics model

1 Introduction

In recent years, magnesium alloys have drawn much industrial and scientific interest due to their excellent properties, such as low density, high specific strength and high specific rigidity [1–5]. Magnesium alloys are commonly produced by hot forming process because of the poor workability at room temperature owing to the hexagonal closed-packed (HCP) crystal structure. As one of the most important microstructural evolution mechanisms in hot processing, dynamic recrystallization (DRX) is beneficial to obtaining fine grains structure, eliminating defects and improving mechanical properties for magnesium alloys [6,7]. Therefore, it is of great practical importance to understand the relationship between the thermal-mechanical parameters and DRX behavior of magnesium alloys during hot processing. In the past, some DRX kinetics models have been proposed for different magnesium alloys. Although there are differences in parameters and forms in these models, they are all on the basis of Avrami function. QUAN et al [5] described the microstructure evolution due to DRX for AZ80 magnesium alloy by the modified Avrami

equation of $X_{\text{DRX}}=1-\exp\{-[(\varepsilon-\varepsilon_c)/\varepsilon^*]^m\}$, where ε_c is the critical strain; ε^* is the strain for maximum softening rate; m is the Avrami constant. In this model, ε_c and ε^* are considered functions of dimensionless parameter, Z/A . Furthermore, the accuracy of the proposed kinetics model was validated by the microstructure graphs. LIU et al [8] proposed a new DRX kinetics model for AZ31B alloy, which is expressed as $X_{\text{DRX}}=[1+k_v^{1-(\varepsilon-\varepsilon_c)/(\varepsilon_{0.5}-\varepsilon_c)}]^{-1}$. In this model, ε_c is the critical strain; $\varepsilon_{0.5}$ is the strain for 50% DRX; k_v is a constant related to the velocity of DRX. According to this model, the DRX development of AZ31B alloy was divided into three phases of slow-beginning, rapid-increasing and slow-rising-to-balance. However, limited investigations have been addressed regarding for the dynamic recrystallization behavior of AZ91D alloy.

The aim of the present work is to investigate the flow behavior and dynamic recrystallization behavior of an as-cast AZ91D alloy by applying the hot compression tests at different temperatures and strain rates. The kinetics model of DRX is established to predict the microstructural evolution of the recrystallized grains. The validity of the proposed DRX kinetics equations is confirmed by the microstructure observation.

2 Experimental

The experimental material was the commercial AZ91D cast rod with dimensions of d 70 mm \times 350 mm, and its chemical composition (mass fraction) was 8.83% Al, 0.578% Zn, 0.175% Mn, 0.1% Si, 0.005% Fe, 0.005% Cu, 0.002% Ni, balance Mg. Cylindrical compression specimens were cut from the as-cast rod with dimensions of d 8 mm \times 12 mm. The tests were carried out on a Gleeble–1500D thermal simulator at temperatures from 220 to 380 °C and strain rates from 0.001 to 1 s⁻¹ with a height reduction of 60%. Specimens were heated to the predetermined temperature and then held isothermally for 180 s. The specimens were water-quenched immediately after deformation and were sectioned perpendicular to the longitudinal compression axis for microstructure observation by optical microscopy (OM) technique. The cutting surface was processed by normal preparing grinding and polishing process, and then was etched with a picric acid etchant.

3 Results and discussion

3.1 Initial microstructure

The initial microstructure of AZ91D alloy is shown

in Fig. 1. The cast structure consisted of dominant α -Mg and an amount of β -Mg₁₇Al₁₂ phases along the grain boundaries, and the average grain size was determined to be 95 μ m approximately.

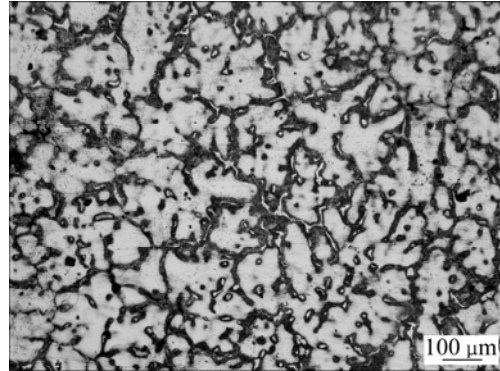


Fig. 1 Initial microstructure of AZ91D alloy

3.2 Flow behavior

The true stress–true strain curves obtained under different conditions are shown in Fig. 2. It is observed that the flow stress firstly increases severely to the peak value and then decreases gradually to steady-state stress as the strain increases. This flow behavior is a typical DRX softening behavior accompanied by work hardening. It is also revealed that the peak stress, critical

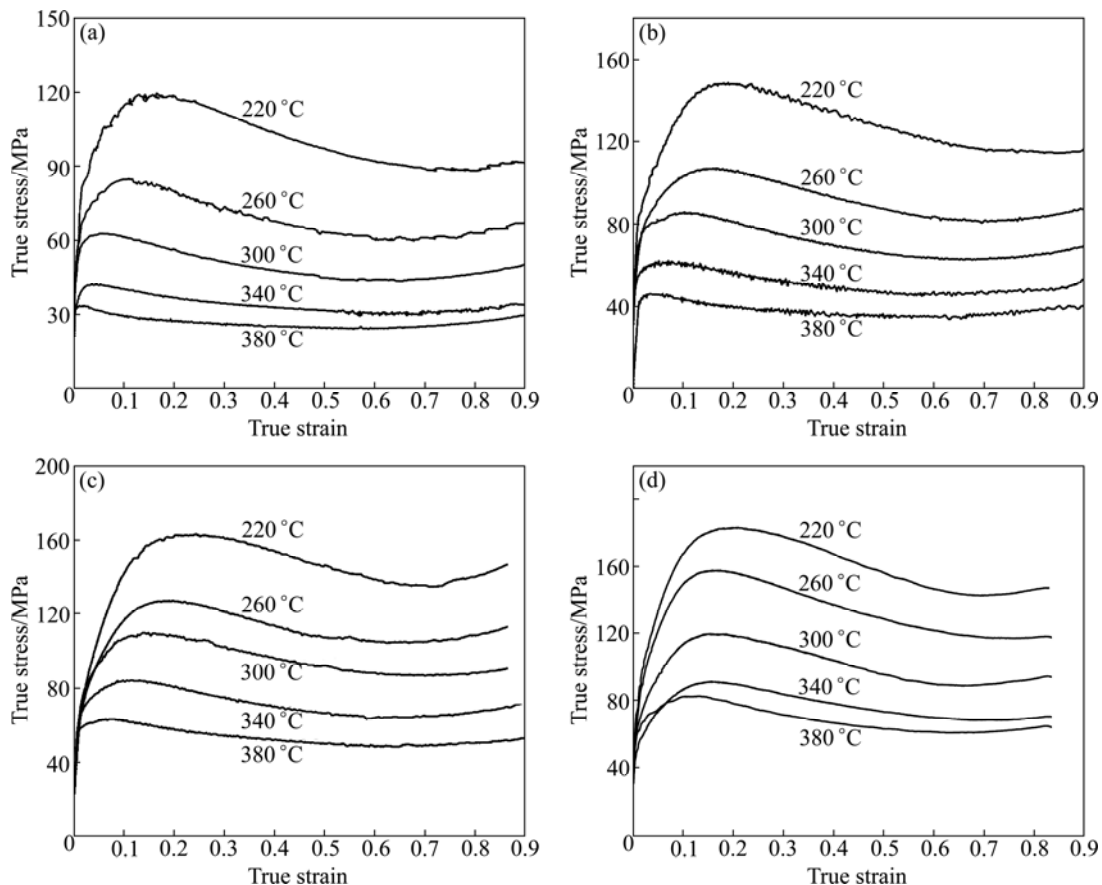


Fig. 2 Typical true stress–true strain curves for AZ91D alloy under various deformation conditions: (a) $\dot{\epsilon} = 0.001$ s⁻¹; (b) $\dot{\epsilon} = 0.01$ s⁻¹; (c) $\dot{\epsilon} = 0.1$ s⁻¹; (d) $\dot{\epsilon} = 1$ s⁻¹

stress, and steady-state stress increase with decreasing temperature and increasing strain rate, indicating that the flow behavior of AZ91D alloy was sensitive to temperature and strain rate. The previous researches on AZ31 magnesium alloys reported by LIU et al [9] and FATEMI-VARZANEH et al [10] also exhibited the typical DRX behavior.

3.3 Kinetics model of dynamic recrystallization

3.3.1 Models for main strains

A typical hardening rate ($\theta=d\sigma/d\varepsilon$) versus flow stress (σ) plot obtained at 220 °C and 0.001 s^{-1} is shown in Fig. 3. It can be obviously seen that the θ - σ plot is divided into three segments. Segment I begins from initial stress to the critical stress (σ_c), where the value of θ decreases sharply. Segment II indicates the deformation from the onset of DRX (corresponding to σ_c) to the peak stress (σ_p), where θ has positive value with lower slope and decreases slowly to zero. This is due to the interaction of work hardening and DRX softening, and work hardening is not counteracted by the softening. Segment III begins from σ_p to the steady-state stress (σ_s), where DRX is the predominant microstructure evolution mechanism and θ is negative. When the steady-state stress ($\theta=0$) reaches, equilibrium between work hardening and DRX softening is obtained [11].

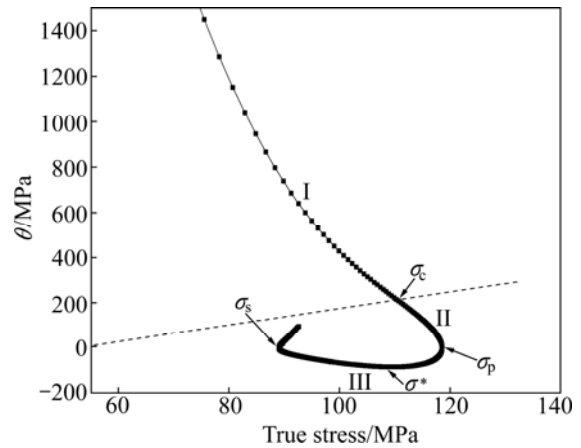


Fig. 3 Typical θ - σ plot obtained at 220 °C and 0.001 s^{-1}

Based on the analysis above, the θ - σ curves at different deformation conditions are plotted in Fig. 4, from which the values of σ_c , σ_p and σ_s could be determined easily. Then the corresponding values of ε_c , ε_p and ε_s would be obtained based on the true stress-true strain data. The strain for maximum softening rate, ε^* (corresponding to σ^* in Fig. 3), is determined when the value of θ reaches the negative peak which corresponds to a valley point in θ - σ plot. The values of ε_c , ε^* and ε_p are often described as functions of dimensionless

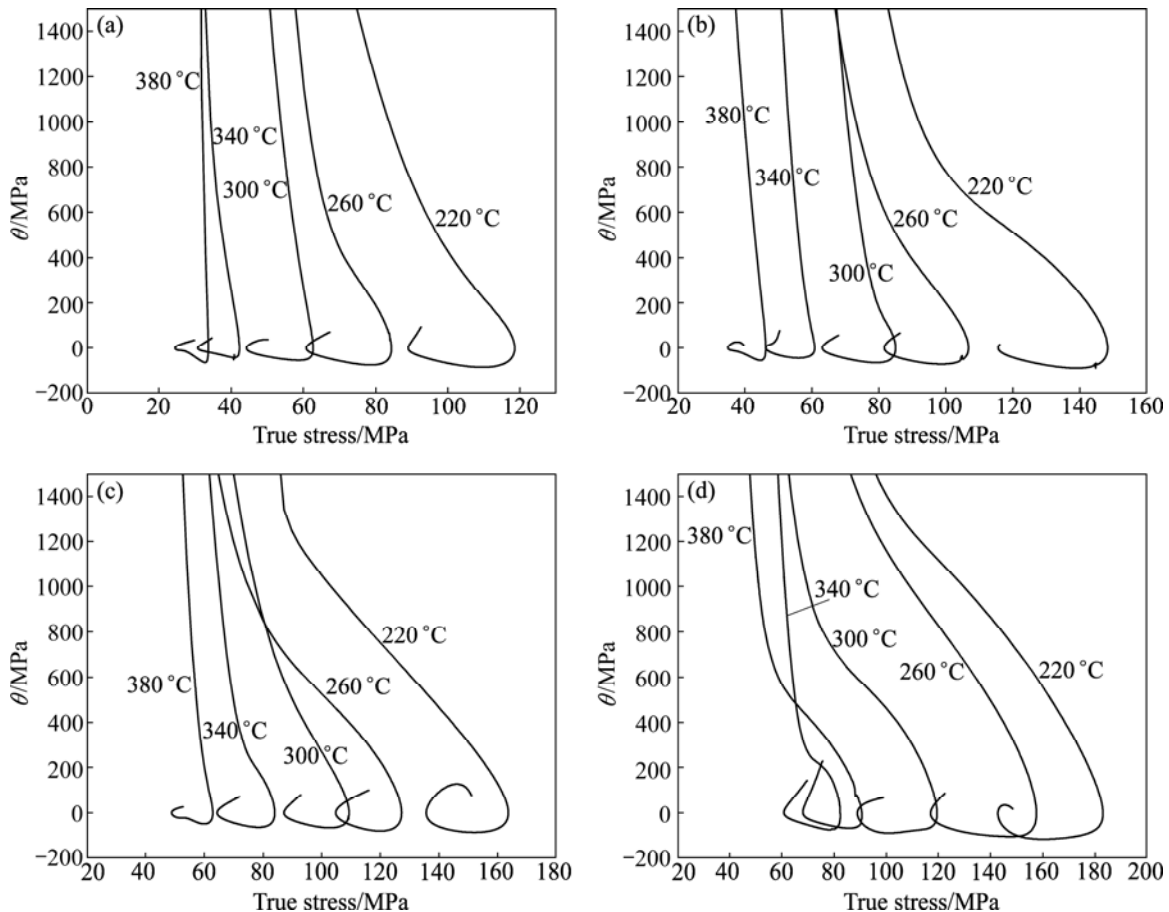


Fig. 4 θ - σ curves at different deformation conditions: (a) $\dot{\varepsilon} = 0.001\text{ s}^{-1}$; (b) $\dot{\varepsilon} = 0.01\text{ s}^{-1}$; (c) $\dot{\varepsilon} = 0.1\text{ s}^{-1}$; (d) $\dot{\varepsilon} = 1\text{ s}^{-1}$

parameter of Z/A [5,12,13], as shown in Fig. 5. The simplified forms are expressed as Eqs. (1)–(3). The relationship between ε_c and ε_p can be usually represented as $\varepsilon_c = k\varepsilon_p$, and the values of k range from 0.2128 to 0.6667 in this study. It was reported from the previous researches that the coefficient values of k were various for different materials. QUAN et al [5] and KIM et al [14] summarized that the values of k were 0.270–0.522 and 0.60–0.70 for AZ80 alloy and AISI 304 stainless steel, respectively. And the values of k were determined to be 0.81 for AZ31B alloy by LIU et al [8].

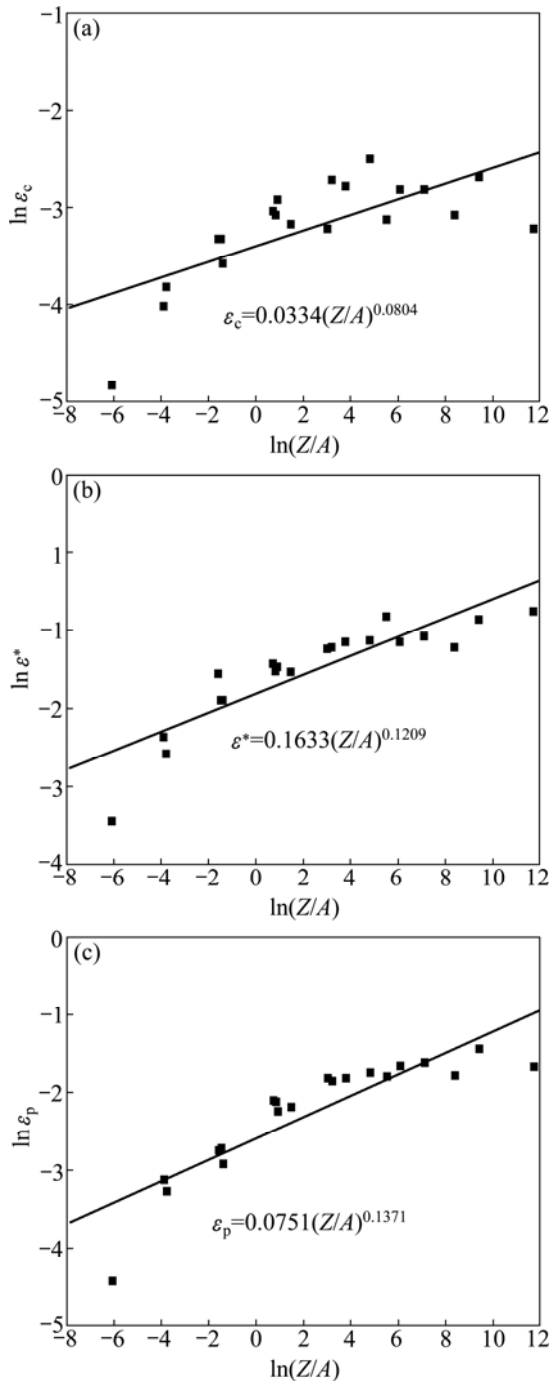


Fig. 5 Relationship of dimensionless parameter, Z/A , with ε_c (a), ε^* (b) and ε_p (c)

$$\varepsilon_c = 0.0334(Z/A)^{0.0804} \quad (1)$$

$$\varepsilon^* = 0.1633(Z/A)^{0.1209} \quad (2)$$

$$\varepsilon_p = 0.0751(Z/A)^{0.1371} \quad (3)$$

where Z is the Zener-Hollomon parameter,

$$Z = \dot{\varepsilon} \cdot \exp\left(\frac{181980}{8.31T}\right)$$

and A is the structure factor ($A = 1.59 \times 10^{14}$), which were reported in the work [15].

3.3.2 Kinetics model of DRX

The onset of DRX depends on the density of the dislocations. When dislocations of the deformed alloy increase and accumulate to an extent that at a critical strain in hot process, DRX nucleus would form at original grain boundaries firstly. When the steady-state flow reaches, the full evolution of dynamic recrystallization occurs and complete DRX grains would keep equiaxed shape and constant size. The evolution of microstructure due to DRX can be predicted by the modified Avrami type equation [12]:

$$X_{\text{DRX}} = 1 - \exp\left\{-k \left[\frac{\varepsilon - \varepsilon_c}{\varepsilon^*}\right]^n\right\} \quad (4)$$

where X_{DRX} is the volume fraction of DRX grains; ε^* is the strain for the maximum softening rate; ε_c is the critical strain; k and n are material constants.

The flow stress of materials characterized by DRX can also be expressed as [8]

$$\sigma - \sigma_p = -X_{\text{DRX}}(\sigma_p - \sigma_s) \quad (5)$$

where X_{DRX} is the DRX volume fraction; σ_p and σ_s are the peak stress and steady-state stress, respectively. So, Eq. (5) can also be written by

$$X_{\text{DRX}} = \frac{\sigma - \sigma_p}{\sigma_s - \sigma_p} \quad (6)$$

Then k and n under various conditions could be obtained by regression analysis. The values of $\ln k$ and $\ln n$ can be described as a quadratic function of $\ln(Z/A)$, and the fitting coefficients are 0.965 and 0.931, respectively. Thus, the kinetic model of DRX is as follows:

$$X_{\text{DRX}} = 1 - \exp\left\{-k \left[\frac{\varepsilon - \varepsilon_c}{\varepsilon^*}\right]^n\right\} \quad (7)$$

$$k = \exp[-1.37309236 + 0.00745888 \times \ln(Z/A) + 0.02248822 \times \ln(Z/A)^2] \quad (8)$$

$$n = \exp[0.7448719 + 0.09481055 \times \ln(Z/A) - 0.0054608 \times \ln(Z/A)^2] \quad (9)$$

The curves of DRX kinetics model at various conditions are shown in Fig. 6 according to Eqs. (1), (2) and (7–9). It can be observed that the volume fraction of

DRX grains increases as the strain increases and the evolution exhibits “slow-rapid-slow” growth trend in terms of S-curves [16]. At a given strain, the volume fraction of DRX grains is much higher at higher temperatures and lower strain rates. Meanwhile, the influence of temperature on the DRX evolution is more pronounced at lower strain rate. This could be due to the increased mobility of grain boundaries with the decrease of strain rate and the increase of temperature. The similar development processes of DRX were also reported from other investigations. FATEMI-VARZANEH et al [10] indicated that the amount and the size of DRX grains for AZ31 increased as Zener-Hollomon parameter decreased, and the evolution of recrystallized grains was observed to increase with increasing strain in a sigmoidal form. QUAN et al [5] researched the DRX behavior of AZ80 and revealed that as deformation temperature increased, more deformed metal transformed to recrystallized microstructure and all the recrystallized grains tended to be more homogeneous.

3.4 Microstructure observation

Microstructure observation was conducted to validate the accuracy of the proposed DRX kinetics model. The DRX evolution at 380 °C and 0.01 s⁻¹ with various strains is shown in Fig. 7. It is revealed from

Fig. 7(a) that at a strain of 0.1, only some newly formed DRX grains occur at original grain boundaries and around the eutectic β phases, which forms a “necklace” type microstructure. It is also found that the DRX grains formed around the eutectic β phases are much finer than those formed at original grain boundaries, which is similar to the investigation on AZ91 alloy reported by XU et al [17]. It was demonstrated that during heating and holding process before compression deformation, a lot of β compounds have already precipitated in Al-rich regions around the massive eutectic β phases at original grain boundaries. During the compression deformation, the β precipitates were crushed into a large number of small blocks. They are effective in retarding the growth of DRX grains, resulting in remarkable grain refinement near β phases. At a strain of 0.36, more fine DRX grains occur at coarse grain boundaries as well as the core of coarse grains (Fig. 7(b)). At a strain of 0.6, as shown in Fig. 7(c), almost all coarse original grains are replaced by the new fine DRX grains. It is observed from Fig. 7(d) that as the strain increases to 0.9, the microstructure exhibits a full evolution of DRX structure and the DRX grain size remains constant. In addition, from the comparison of deformed microstructures (Figs. 7(a)–(d)) with as-cast structure (Fig. 1), it can be seen that, initial eutectic β phases with net-like distribution at original

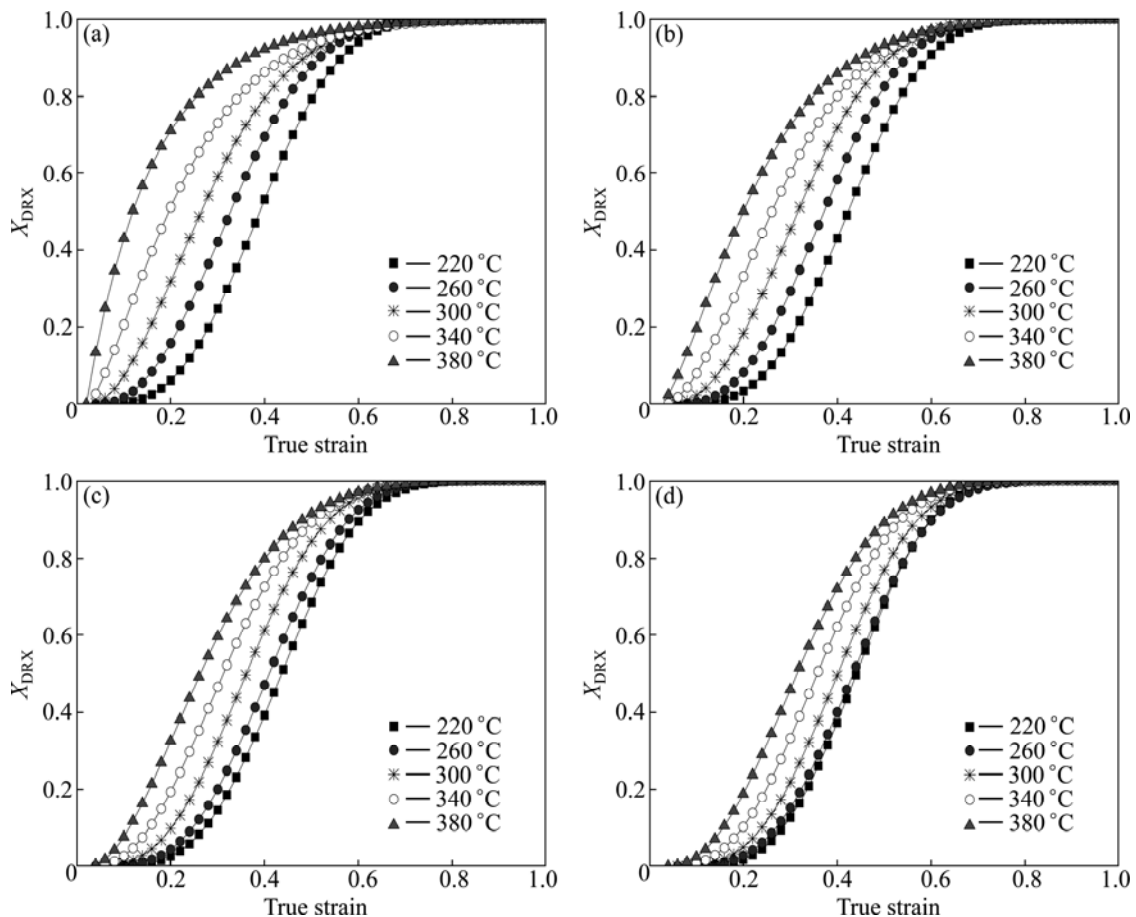


Fig. 6 Curves of DRX kinetics model at various conditions: (a) $\dot{\epsilon} = 0.001 \text{ s}^{-1}$; (b) $\dot{\epsilon} = 0.01 \text{ s}^{-1}$; (c) $\dot{\epsilon} = 0.1 \text{ s}^{-1}$; (d) $\dot{\epsilon} = 1 \text{ s}^{-1}$

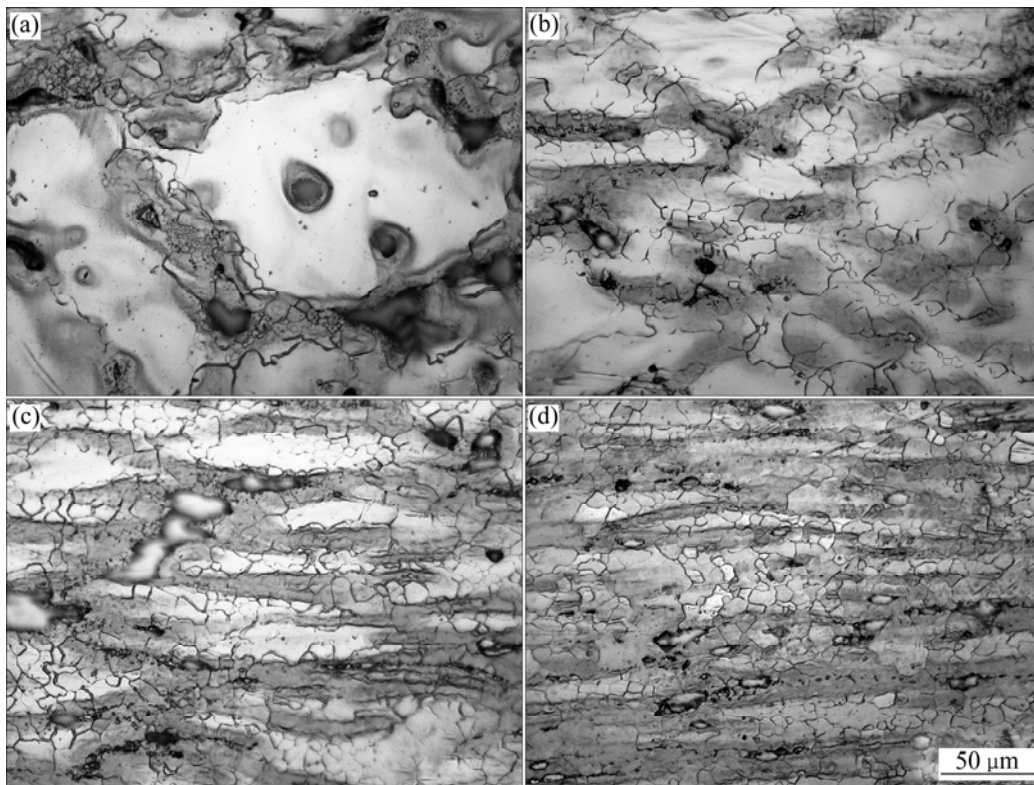


Fig. 7 Microstructures of AZ91D alloy deformed at 380 °C and 0.01 s⁻¹ with different strains: (a) 0.1; (b) 0.36; (c) 0.6; (d) 0.9

grain boundaries have been gradually replaced by smaller blocks of β phases along the horizontal deformation bands. This is because more eutectic β phases precipitate with the development of compression, and the residual β phases would be crushed into a number of small blocks by the shear effect of deformation bands.

The comparison between the proposed DRX kinetics model and the experimental data at 380 °C and 0.01 s⁻¹ is shown in Fig. 8, where the experimental data take the average value of five measured data. It is revealed that the DRX volume fraction of the experimental results is in good agreement with the predicted data. This indicates that the proposed kinetics model can give an accurate estimate of DRX behavior of AZ91D alloy during hot deformation. Furthermore, the average grain sizes of newly formed DRX grains are determined to be 8.33, 9.86, 9.95 and 9.94 μm at various strains of 0.1, 0.36, 0.6 and 0.9 by using a mean linear intercept method, which reveals the visible grain refinement for as-cast AZ91D alloy after hot compression deformation. It is also indicated that as the strain increases from 0.1 to 0.6, more and more DRX grains nucleate and grow gradually. When the strain exceeds 0.6, a full evolution of DRX structure exhibits and the average grain size keeps constant, which corresponds to the fully recrystallized stage at 380 °C and 0.01 s⁻¹ in Fig. 6(b).

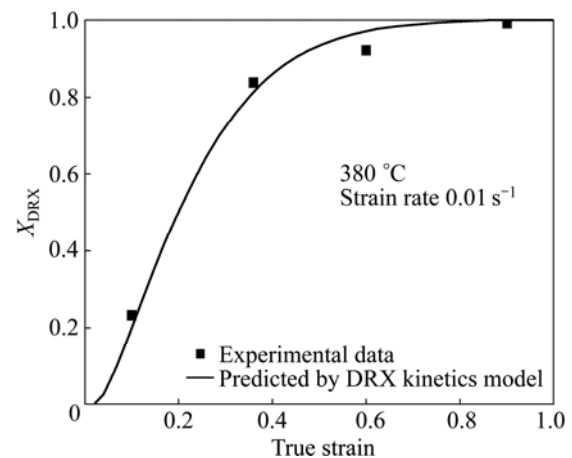


Fig. 8 Comparison between predicted and experimental data

4 Conclusions

- 1) The flow behavior of as-cast AZ91D alloy exhibits a typical dynamic recrystallization softening, which is affected by temperature and strain rate.
- 2) The evolution of DRX is sensitive to temperature and strain rate and DRX grains easily occur at higher temperatures and lower strain rates.
- 3) The DRX kinetics equation of AZ91D alloy can be represented as

$$X_{\text{DRX}} = 1 - \exp \left\{ -k \left[\frac{\varepsilon - \varepsilon_c}{\varepsilon^*} \right]^n \right\}$$

$$k = \exp[-1.37309236 + 0.00745888 \times \ln(Z/A) + 0.02248822 \times \ln(Z/A)^2]$$

$$n = \exp[0.7448719 + 0.09481055 \times \ln(Z/A) - 0.0054608 \times \ln(Z/A)^2]$$

$$\varepsilon_c = 0.0334(Z/A)^{0.0804}$$

$$\varepsilon^* = 0.1633(Z/A)^{0.1209}$$

$$\varepsilon_p = 0.0751(Z/A)^{0.1371}$$

4) Microstructure observation indicates that the proposed kinetics model of DRX is basically consistent with the experimental data. An accurate estimate for the DRX volume fraction of AZ91D can be given by the proposed DRX kinetics model.

References

- [1] CHEN Shu-ying, CHANG Guo-wei, HUANG Yu-duo, LIU Sheng-yang. Effects of melt temperature on as-cast structure and mechanical properties of AZ31B magnesium alloy [J]. Journal of Materials Processing Technology, 2013, 23(6): 1602–1609.
- [2] SHI Bao-liang, LUO Tian-jiao, WANG Jing, YANG Yuan-sheng. Hot compression behavior and deformation microstructure of Mg–6Zn–1Al–0.3Mn magnesium alloy [J]. Transactions of Nonferrous Metals Society of China, 2013, 23(9): 2560–2567.
- [3] WANG Li-fei, HUANG Guang-sheng, LI Hong-cheng, ZHANG Hua. Influence of strain rate on microstructure and formability of AZ31B magnesium alloy sheets [J]. Transactions of Nonferrous Metals Society of China, 2013, 23(4): 916–922.
- [4] SEVIK H, AÇIKGÖZ S, CAN KURNAZ S. The effect of tin addition on the microstructure and mechanical properties of squeeze cast AM60 alloy [J]. Journal of Alloys and Compounds, 2010, 508(1): 110–114.
- [5] QUAN Guo-zheng, SHI Yu, WANG Yi-xin, KANG Beom-Soo, KU Tae-Wan, SONG Woo-Jin. Constitutive modeling for the dynamic recrystallization evolution of AZ80 magnesium alloy based on stress–strain data [J]. Materials Science and Engineering A, 2011, 528: 8051–8059.
- [6] AL-SAMMAN T, GOTTSTEIN G. Dynamic recrystallization during high temperature deformation of magnesium [J]. Materials Science and Engineering A, 2008, 490(1–2): 411–420.
- [7] XU Yan, HU Lian-xi, DENG Tai-qing, YE Lei. Hot deformation behavior and processing map of as-cast AZ61 magnesium alloy [J]. Materials Science and Engineering A, 2013, 559: 528–533.
- [8] LIU J, CUI Z, RUAN L. A new kinetics model of dynamic recrystallization for magnesium alloy AZ31B [J]. Materials Science and Engineering A, 2011, 529: 300–310.
- [9] LIU J, CUI Z, LI C. Modelling of flow stress characterizing dynamic recrystallization for magnesium alloy AZ31B [J]. Computational Materials Science, 2008, 41(3): 375–382.
- [10] FATEMI-VARZANEH S M, ZAREI-HANZAKI A, BELADI H. Dynamic recrystallization in AZ31 magnesium alloy [J]. Materials Science and Engineering A, 2007, 456(1–2): 52–57.
- [11] XU Yan, HU Lian-xi, SUN Yu. Deformation behaviour and dynamic recrystallization of AZ61 magnesium alloy [J]. Journal of Alloys and Compounds, 2013, 580: 262–269.
- [12] LÜ B J, PENG J, SHI D W, TANG A T, PAN F S. Constitutive modeling of dynamic recrystallization kinetics and processing maps of Mg–2.0Zn–0.3Zr alloy based on true stress–strain curves [J]. Materials Science and Engineering A, 2013, 560: 727–733.
- [13] JI Guo-liang, LI Fu-guo, LI Qing-hua, LI Hui-qu, LI Zhi. Research on the dynamic recrystallization kinetics of Aermet100 steel [J]. Materials Science and Engineering A, 2010, 527: 2350–2355.
- [14] KIM Sung-II, LEE Youngseog, LEE Duk-Lak, YOO Yeon-Chul. Modeling of AGS and recrystallized fraction of microalloyed medium carbon steel during hot deformation [J]. Materials Science and Engineering A, 2003, 355(1–2): 384–393.
- [15] XU Yan, HU Lian-xi, SUN Yu. Hot deformation behavior and microstructure evolution of as-cast AZ91D magnesium alloy without pre-homogenization treatment [J]. Rare Metals, 2013, 32(4): 338–346.
- [16] GUO Q, YAN H G, ZHANG H, CHEN Z H, WANG Z F. Behaviour of AZ31 magnesium alloy during compression at elevated temperatures [J]. Materials Science and Technology, 2005, 21(11): 1349–1354.
- [17] XU S W, KAMADO S, MATSUMOTO N, HONMA T, KOJIMA Y. Recrystallization mechanism of as-cast AZ91 magnesium during hot compression deformation [J]. Materials Science and Engineering A, 2009, 527(1–2): 52–60.

铸态 AZ91D 镁合金的动态再结晶动力学

徐岩^{1,2}, 胡连喜¹, 孙宇¹

1. 哈尔滨工业大学 材料科学与工程学院, 哈尔滨 150001;

2. 北华大学 机械工程学院, 吉林 132021

摘要: 在温度为 220~380 °C 和应变速率为 0.001~1 s⁻¹ 的条件下进行等温热压缩, 研究铸态 AZ91D 镁合金的变形行为和动态再结晶行为。讨论变形温度和应变速率对动态再结晶行为的影响。结果表明, 动态再结晶晶粒的形核和长大极易在高温和低应变速率的条件下发生。为预测动态再结晶的演变过程, 在真实应力—应变曲线数据的基础上, 提出 AZ91D 镁合金的动态再结晶动力学模型。该模型揭示动态再结晶的体积分数随着真实应变的增加而增加, 其增长趋势呈典型的“S”曲线。通过对比发现由动力学模型所预测的结果和微观组织观测的数据具有很好的一致性, 验证了所建立的 AZ91D 镁合金动态再结晶动力学模型的准确性。

关键词: AZ91D 镁合金; 压缩; 流变行为; 动态再结晶行为; 动力学模型